ELSEVIER

Journal of Structural Geology 26 (2004) 1025–1041

JOURNAL OF STRUCTURAL GEOLOGY

www.elsevier.com/locate/jsg

Structural and mechanical controls on intrusion-related deposits of the Tombstone Gold Belt, Yukon, Canada, with comparisons to other vein-hosted ore-deposit types

Julian R. Stephens[a,*], John L. Mair[b], Nicholas H.S. Oliver[a], Craig J.R. Hart[b,c], Timothy Baker[a]

[a]*Economic Geology Research Unit (EGRU), School of Earth Sciences, James Cook University, Queensland 4811, Australia*
[b]*Centre for Global Metallogeny, Department of Geology and Geophysics, The University of Western Australia, Nedlands, Western Australia 6907, Australia*
[c]*Yukon Geology Program, Box 2703 (K-10), Whitehorse, Yukon Territory, Canada, Y1A 2C6*

Received 3 November 2002; received in revised form 11 April 2003; accepted 5 June 2003

Abstract

Intrusion-related gold deposits at the Clear Creek, Scheelite Dome and Dublin Gulch properties of the Tombstone Gold Belt (TGB), Yukon Territory have dominantly E-striking, steeply dipping, auriferous quartz extension veins within intrusions. In adjacent metasedimentary rocks gold is hosted in subvertical NW- to NNW-striking sinistral faults as veins and breccias, in E-striking extension veins and locally in E- to ENE-striking fault veins. These structural relationships indicate low magnitude, broadly E–W-directed shortening and N–S extension during stock emplacement and gold mineralisation at ~92 Ma.

The lack of any deviation or deflection of the extension vein orientations in the country rocks, with respect to their orientation within the stocks, indicates consistent stress trajectories in both rock types. These TGB deposits formed at 5–8 km depth, where mean and differential stresses may be greater in magnitude than in shallower porphyry environments. Many porphyry systems feature magmatic-related stresses that dominated the local stress field, with more variable vein orientations the result. Conversely, orogenic gold systems usually exhibit strong dimensionality in vein orientations. Fault-hosted mineralisation in metasedimentary rocks of the TGB deposits in this study is comparable in geometry, but generally smaller in size than in many orogenic gold systems. Intrusion-related systems of the TGB exhibit intermediate structural styles of mineralisation that provide a useful bridge in understanding the diversity of mechanically controlled structural styles in otherwise mostly unrelated gold deposit types.

Keywords: Intrusion-related; Gold; Veins; Mechanical; Stress; Yukon

1. Introduction

Intrusion-related gold deposits in the Tombstone Gold Belt (TGB) of Yukon, Canada, are characterised by sheeted mineralised veins within granitoid bodies and fault-veins, breccias and replacement/skarn style mineralisation in the country rocks. The TGB gold deposits include Brewery Creek (13.3 Mt at 1.44 g/t Au; Diment and Craig, 1999), Dublin Gulch (99 Mt at 1.1 g/t Au; Smit et al., 1996) and numerous other properties in advanced stages of exploration such as Scheelite Dome and Clear Creek (~40 Mt at > 0.3 g/t Au; Coombes 1996; recent drill intersections include 34.9 m at 2.0 g/t Au and 31.8 m at 2.3 g/t Au; Stephens and Weekes, 2001). The TGB forms the eastern part of the larger Tintina Gold Province that spans central Yukon and east-central Alaska (Hart et al., 2002). Other deposits of the Tintina Gold Province are spatially and temporally related to mid- and Late-Cretaceous plutonic rocks and include Pogo (9.0 Mt at 17.8 g/t Au; Smith et al., 2000), Fort Knox (169 Mt at 0.93 g/t Au; Bakke, 1995) and Donlin Creek (111 Mt at 2.91 g/t Au; Ebert et al., 2000; Fig. 1a) in Alaska. More specifically, Tombstone Gold Belt deposits are associated with ~92 Ma felsic to intermediate intrusions of the Tombstone Plutonic Suite (TPS) that form a belt spanning >600 km across central Yukon and eastern Alaska (Fig. 1a and b; Mortensen et al., 2000). Westernmost TPS intrusions have been offset by ~450 km of dextral displacement along the Tintina Fault to their current location where they underlie the Fairbanks mineral district of east-central Alaska (Fig. 1a).

Recent studies on deposits of the TGB, and similar mineralised systems worldwide, have recognised that these deposits comprise a distinct class of intrusion-related gold

* Corresponding author. Tel.: +61-7-4728-5220; fax: +61-7-4725-1501.
E-mail address: julian.stephens@jcu.edu.au (J.R. Stephens).

0191-8141/$ - see front matter © 2004 Elsevier Ltd. All rights reserved.
doi:10.1016/j.jsg.2003.11.008

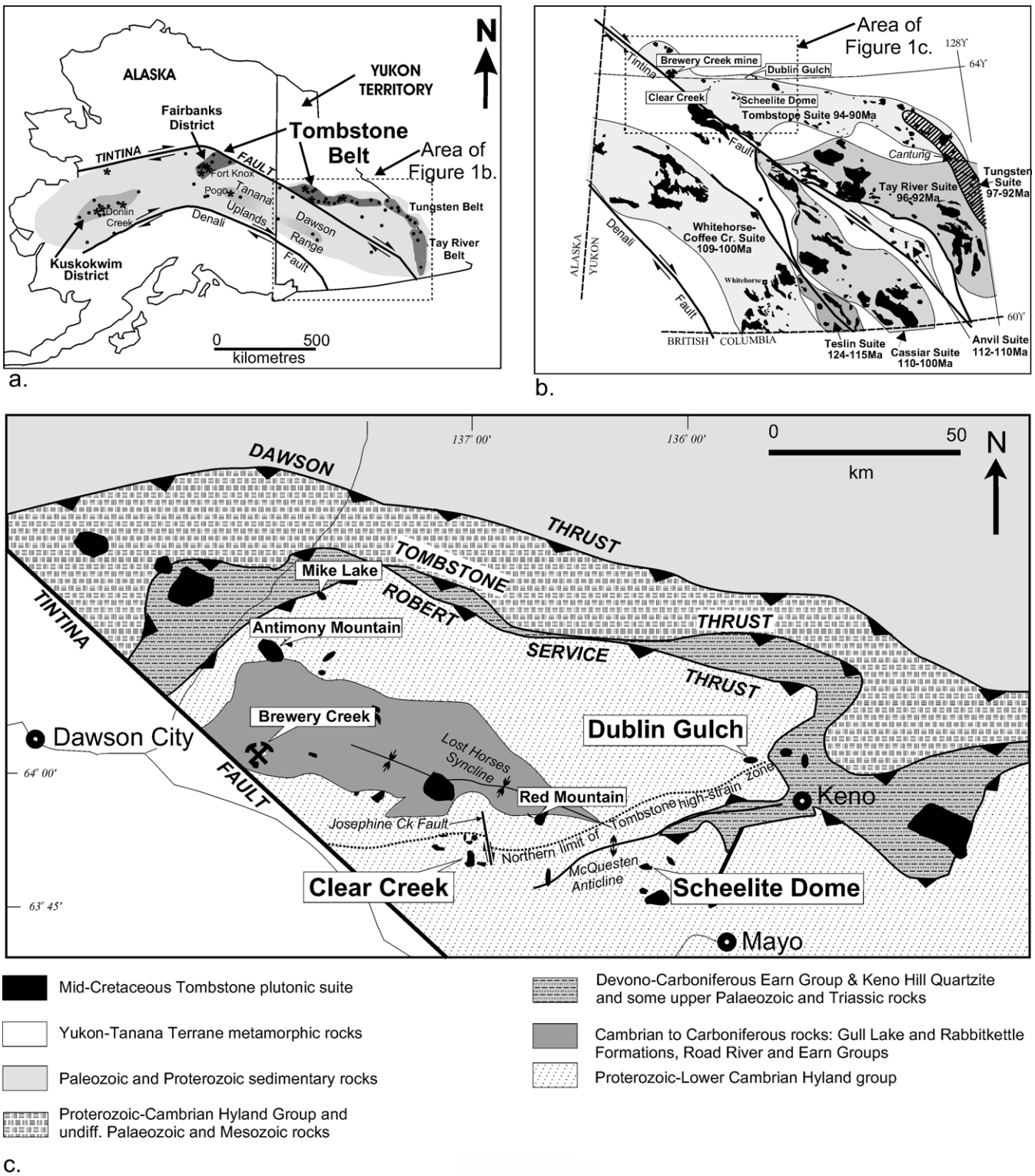

Fig. 1. (a) Simplified map of the Tintina Gold Province of Alaska and Yukon Territory, Canada showing locations of deposits (stars), significant occurrences (dots) and main regions of intrusion-related gold mineralisation. (b) Map of the main intrusive suites in the Yukon Territory (modified from Mortensen et al., 2000). (c) Simplified geological map of the western Selwyn Basin showing the main tectonic features, the location of the study areas (large boxes) and other important TGB deposits and prospects (small boxes) (modified from Murphy, 1997).

systems (e.g. McCoy et al., 1997; Sillitoe and Thompson, 1998; Thompson et al., 1999; Lang et al., 2000; Thompson and Newberry, 2000). These systems are characterised by spatial and temporal relationships to moderately reduced, felsic intrusions that occur in cratonic margins in landward or back-arc positions relative to continental arcs, or within continental collisional settings (Thompson et al., 1999). The mineralisation is characterised by a metal suite that includes Au–Bi–Te–As (±W, Mo, Sb). The structural controls on these deposits, although important in their genesis, are poorly understood (Thompson and Newberry, 2000).

This paper describes the structural and mechanical controls associated with TGB intrusion-related deposits at Clear Creek, Dublin Gulch and Scheelite Dome in Yukon. These deposits exhibit similar orientations of mineralised faults and veins across the belt. However, unlike orogenic gold systems (e.g. Groves et al., 1998), no regional-scale mineralisation controlling faults or shear zones are recognised. Although all of the TGB deposits have spatial and temporal relationships to intrusions, the deposits differ from typical porphyry gold systems in that they have this consistent similarity in vein and fault orientations over hundreds of kilometres. Structural comparisons of intrusion-related gold mineralisation are therefore made with porphyry and orogenic gold systems and a structural exploration model for TGB and similar systems is developed.

2. Tectonic setting

2.1. The northern Canadian Cordillera

The Canadian Cordillera is the product of a variety of tectonic processes acting upon and adjacent to the continental margin from the Mesoproterozoic to the present, although it remained in a passive margin setting throughout much of this time (Gabrielse and Yorath, 1991) During the Late Jurassic to Early Cretaceous accretion of large exotic superterranes resulted in intense metamorphism, associated plutonism and crustal thickening along the continental margin. Subsequent extensive magmatism in the northern Canadian Cordillera during the Early- and middle-Cretaceous resulted from easterly-directed subduction of the Farallon plate (Engebretson et al., 1985). In Yukon, the Whitehorse–Coffee Creek, Anvil and Cassiar plutonic suites were generated by arc-trench-related magmatism (Engebretson et al., 1985; Mortensen et al., 2000). A series of slightly orogen-oblique magmatic belts, including the TPS, stepped progressively northward between ~99 and ~89 Ma (Mortensen et al., 2000), possibly in response to ongoing subduction of the Farallon plate (Goldfarb et al., 2000).

2.2. The western Selwyn Basin

From the latest Neoproterozoic to Carboniferous, dominantly clastic sedimentary rocks were deposited in an off-shelf setting of the Selwyn basin (Gordey and Anderson, 1993). These rocks are transitional northwards and eastwards into coeval shelf carbonate and clastic shelf sedimentary rocks of the Mackenzie Platform (Gordey and Anderson, 1993). In central Yukon, these rocks were deformed in a northerly-directed, fold-and-thrust belt in the Late Jurassic to Early Cretaceous (Murphy, 1997), with the Dawson, Tombstone and Robert Service thrusts developing across the northern part of the basin (Fig. 1c). The Robert Service and Tombstone thrusts are generally considered to be coeval. However, it has also been noted that that the Robert Service Thrust is deformed by ductile deformation in the hanging-wall of the Tombstone Thrust (Murphy, 1997). Rocks in the hanging-wall of the Tombstone Thrust were subjected to intense ductile deformation between the Late Jurassic and Early Cretaceous that produced inclined folds and subhorizontal foliations at lower greenschist facies (Murphy, 1997; Stephens et al., 2000). This regional-scale zone of highly deformed rocks, termed the Tombstone high-strain zone (THSZ), was subsequently folded by the broad, regional, upright, gently west-plunging McQuesten Antiform. The geometry on the northern limb of the McQuesten Antiform (e.g. at Clear Creek) is a shallowly north-dipping foliation (Murphy, 1997; Stephens et al., 2000), while on the southern limb (e.g. at Scheelite Dome) the main foliation dips moderately south to southeast (Murphy, 1997; Mair et al., 2000). All three study areas are underlain by Neoproterozoic–Cambrian Hyland Group rocks that comprise mostly psammite and phyllite with lesser calcareous rocks (Gordey and Anderson, 1993; Murphy, 1997). TPS intrusions were emplaced into these rocks in the mid-Cretaceous at ~92 Ma and clearly cut all THSZ fabrics (Murphy, 1997; Mortensen et al., 2000).

3. Deposit characteristics

3.1. Introduction

The three deposits selected for this study, Clear Creek, Scheelite Dome and Dublin Gulch, were chosen for their known gold mineralisation and prospects, relatively good exposure and wide range of mineralisation styles All of these deposits are temporally and spatially related to TPS stocks. The TPS granitoids are quartz-bearing, weakly to strongly porphyritic and composed of moderately reduced, metaluminous to slightly peraluminous granite, granodiorite, diorite or quartz monzonite (Gordey and Anderson, 1993; Murphy, 1997; Mortensen et al., 2000). Stocks were emplaced at pressures of between 1 and 2.5 kb (Baker and Lang, 1999; Marsh et al., 2003). In general, the stocks have no discernable fabric derived from ductile flow during intrusion, except within a few metres of some stock margins. Inner contact metamorphic and metasomatic

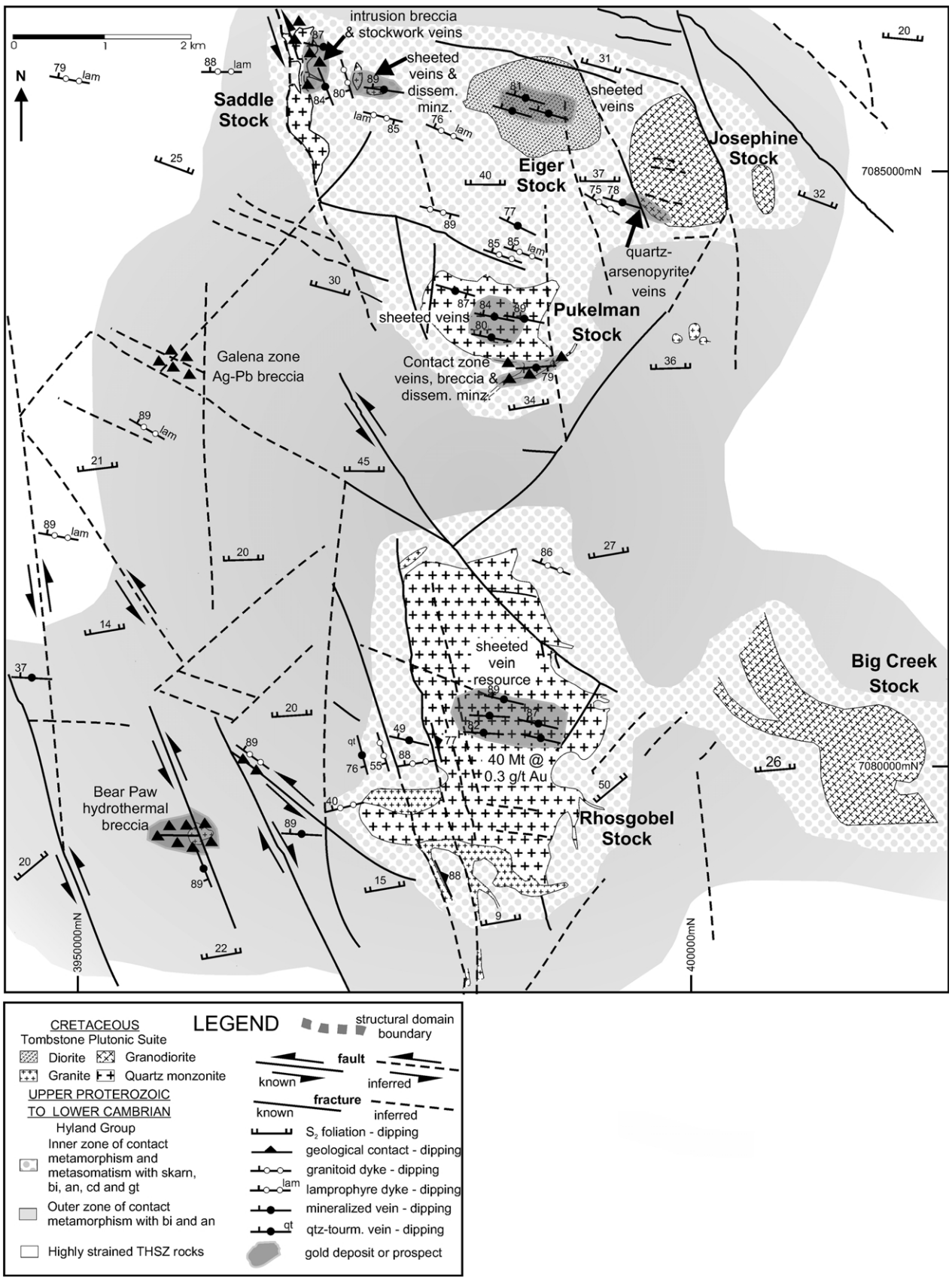

Fig. 2. Simplified geological and structural map of the Clear Creek area showing the zones of significant gold mineralisation (incorporating data from Murphy (1997) and Marsh et al. (1999)).

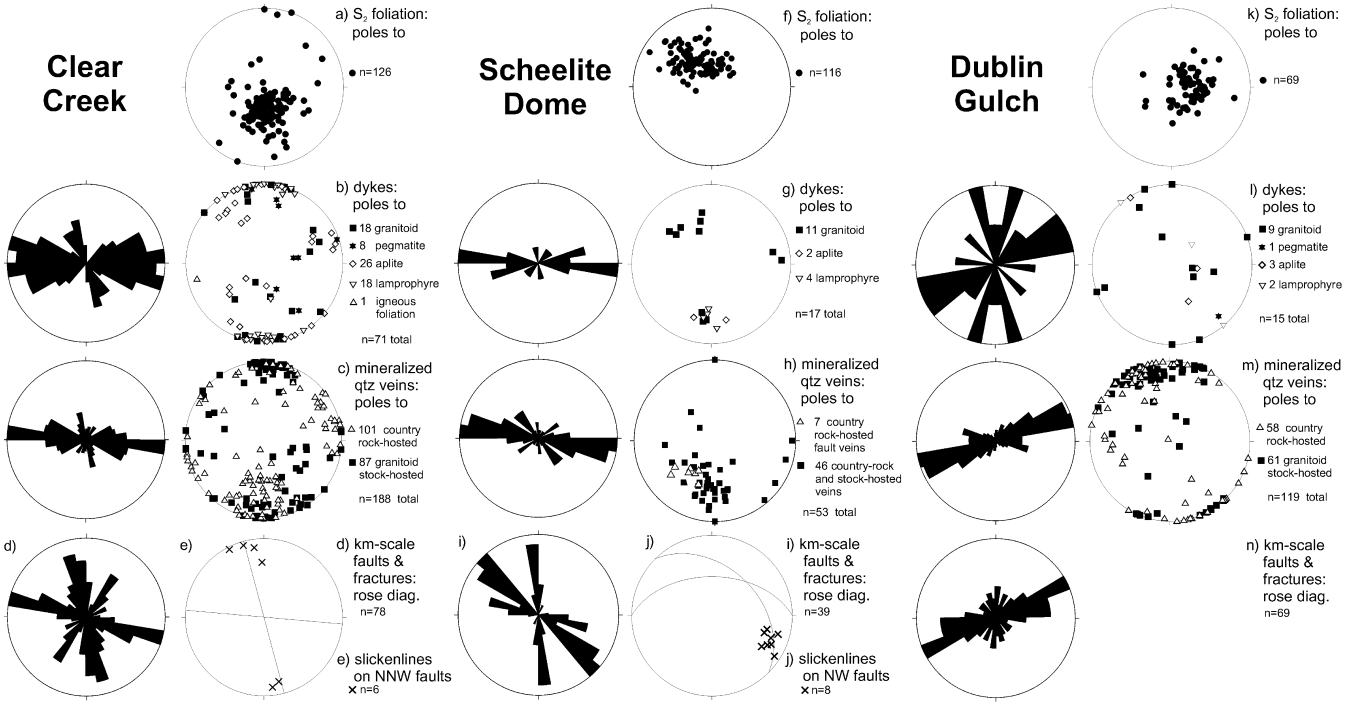

Fig. 3. Rose diagrams and stereonets for the important structural features from the Clear Creek, Scheelite Dome and Dublin Gulch properties.

aureoles are manifest as resistant ridges surrounding the stocks and are ≤500 m in width. They are characterised by intense biotite, andalusite ± garnet growth in pelitic horizons, skarnification of calcareous rocks and partial fabric destruction. Less distinct outer zones of contact metamorphism are characterised by weak biotite and andalusite growth over the regional metamorphic fabric and extend up to 4 gkm from exposed stock margins.

Gold mineralisation occurs in a wide variety of settings in both the country rocks and the granitoid stocks at all properties in this study (Murphy, 1997; Poulsen et al., 1997; Hart et al., 2000). Gold within the stocks is hosted in broadly E-striking, steeply dipping sheeted arrays of extension veins (Poulsen et al., 1997). In adjacent hornfels and distal metasedimentary rocks gold is hosted in moderately to steeply dipping NW- to NNW-striking fault veins and breccias (e.g. Murphy and Héon, 1994; O'Dea et al., 2000; Stephens et al., 2000; Stephens and Weekes, 2001), E-striking extension veins (e.g. Murphy, 1997; Poulsen et al., 1997; Marsh et al., 1999, 2003; O'Dea et al., 2000; Maloof et al., 2001), locally E- to ENE-striking fault veins (e.g. Smit et al., 1996) and skarns (e.g. Mair et al., 2000; O'Dea et al., 2000; Stephens and Weekes, 2001). Most veins are dominantly quartz with lesser K-feldspar, sericite and carbonate and generally have low sulphide (<5%) content (e.g. Poulsen et al., 1997; Marsh et al., 1999; Maloof et al., 2001). Ore minerals include arsenopyrite, pyrite and pyrrhotite with lesser molybdenite, chalcopyrite, bismuthinite, stibnite, sphalerite, gold tellurides and native gold (Marsh et al., 1999; Mair et al., 2000; Maloof et al., 2001; Stephens and Weekes, 2001; J. Mair unpub. data). Vein-related alteration is generally confined to discrete selvages along vein margins and composed of K-feldspar ± sericite ± carbonate in granitic rocks and sericite ± carbonate in the metasedimentary country rocks (Smit et al., 1996; Marsh et al., 1999; O'Dea et al., 2000; Maloof et al., 2001).

Regional structural studies on this area of the TGB include those by Murphy (1997) and Poulsen et al. (1997). Specific studies with structural components have been undertaken by Marsh et al. (1999) and Stephens et al. (2000) on Clear Creek, Hulstein et al. (1999), Mair et al. (2000) and O'Dea et al. (2000) on Scheelite Dome and Templeman-Kluit (1964), Lennan (1983), Hitchens and Orssich (1995) and Smit et al. (1996) on Dublin Gulch. We present detailed structural data including vein, dyke and fault orientations and slickenline trends from these three important TGB deposits. These data are used to constrain the stress field and mechanical failure conditions required for vein formation in order to develop better exploration models for these deposit types.

3.2. Structural characteristics of individual deposits

3.2.1. Clear Creek

At Clear Creek there are six main TPS stocks that range from diorite and granodiorite to the east and quartz monzonite to the west (Fig 2) The Saddle, Pukelman and Rhosgobel stocks crop out in a broad NNW-striking zone (Fig. 2). Sub-vertically dipping granitoid, lamprophyre, pegmatite and aplite dykes strike broadly NNW and E across the area, in addition to a minor, partly foliation

concordant, shallowly north dipping set of sills (Fig. 3a and b).

Auriferous veins hosted within intrusions are steeply dipping and strike almost exclusively E (Fig. 3c; Murphy, 1997; Poulsen et al., 1997; Marsh et al., 1999). In country rocks, however, mineralised veins occur in three main orientations: (1) steeply dipping, E-striking, (2) partly foliation concordant and shallow to moderately N-dipping, and (3) steeply dipping and NNW-striking fault veins/breccias such as the Bear Paw breccia (Fig. 3c; Stephens and Weekes, 2001). The E-striking, steeply dipping vein set shows no variation or deflection in orientation between igneous and country rock hosts.

Kilometre-scale faults and fracture zones in the area occur in three dominant orientations, all of which are steeply dipping, ESE-, NNW- and NE-striking (Fig. 3d). The NNW-striking faults, where mineralised with veins and breccias (Fig. 4c), have mostly small sinistral separations between 1 and 100 m. Evidence for sinistral strike-slip displacement includes stepped, shallowly plunging slickenlines (Fig. 3e), foliation warping and offsets of veins, dykes and metasedimentary rock units. Notably, some of these faults, including the Josephine fault (Murphy, 1997) just to the east of the property, show early apparent dextral offsets. The E-striking structures are dominantly extensional fracture zones with little or no shear displacement and contain the major set of auriferous quartz veins. The NE-striking fault/fracture set contains only rare veins. In general, NNW-striking faults and veins dominate in the western area, with E-striking fracture and sheeted vein zones being more important for gold mineralisation in the eastern part of the property (Fig. 2).

Relationships between the geometry of the granitoid stocks and the fault/fracture network indicate that the faults may have been important in the localisation of stocks. More specifically, the NNW-striking line of quartz monzonite stocks (i.e. Saddle, Pukelman and Rhosgobel) suggests that NNW-striking faults exerted some control on emplacement of these intrusions. In addition, many quartz–monzonite, and dykes of other compositions strike eastwards (cf. Poulsen et al., 1997; Marsh et al., 1999). These data collectively suggest NNW-trending faults were active, even if only to facilitate stock emplacement, synchronously with dilation on the E-striking fracture zones. Mineralised quartz veins also have a similar distribution, with NNW-striking veins occurring generally only in the western part of the property, dominantly within and adjacent to the Saddle and Rhosgobel stocks, and in the Bear Paw breccia zone. Conversely, E-striking mineralised veins occur in both structural domains, with the highest densities in granitoid stocks (e.g. Fig. 3a and b), commonly in association with E-striking dykes.

3.2.2. Scheelite Dome

Two main quartz–monzonite stocks crop out in the Scheelite Dome area (Fig. 5). The Scheelite Dome stock is mostly E–W-striking, with near-foliation concordant, S-dipping north and south contacts. The Morrison Creek stock is N-striking and has steeply dipping contacts. The Scheelite Dome stock and the metasedimentary rocks immediately to the south of it are intruded by many foliation concordant sills and moderate- to steeply N- and S-dipping, E-striking TPS dykes.

Auriferous quartz veins are predominantly hosted within

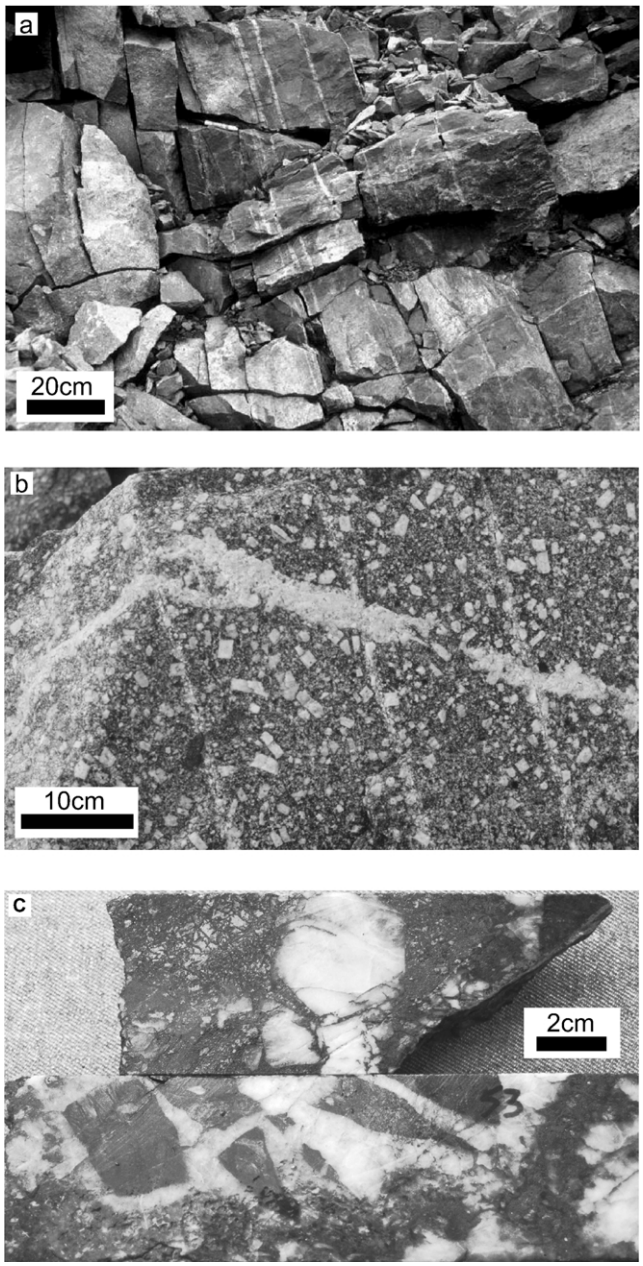

Fig. 4. Photographs of gold mineralised samples from Clear Creek. (a) Typical outcrop of auriferous sheeted veins from the Rhosgobel Stock; near vertical face looking east. (b) Strongly porphyritic quartz monzonite of the Pukelman stock cut by aplite and hairline, evenly spaced auriferous sheeted veins with K-feldspar selvages; near the horizontal face, top is west. (c) Drill-core sample of hydrothermal breccia from the Bear Paw zone with angular fragments of psammo–pelitic Hyland Group in a matrix of quartz–K-feldspar–sulphide veins. This sample grades 23 g/t Au.

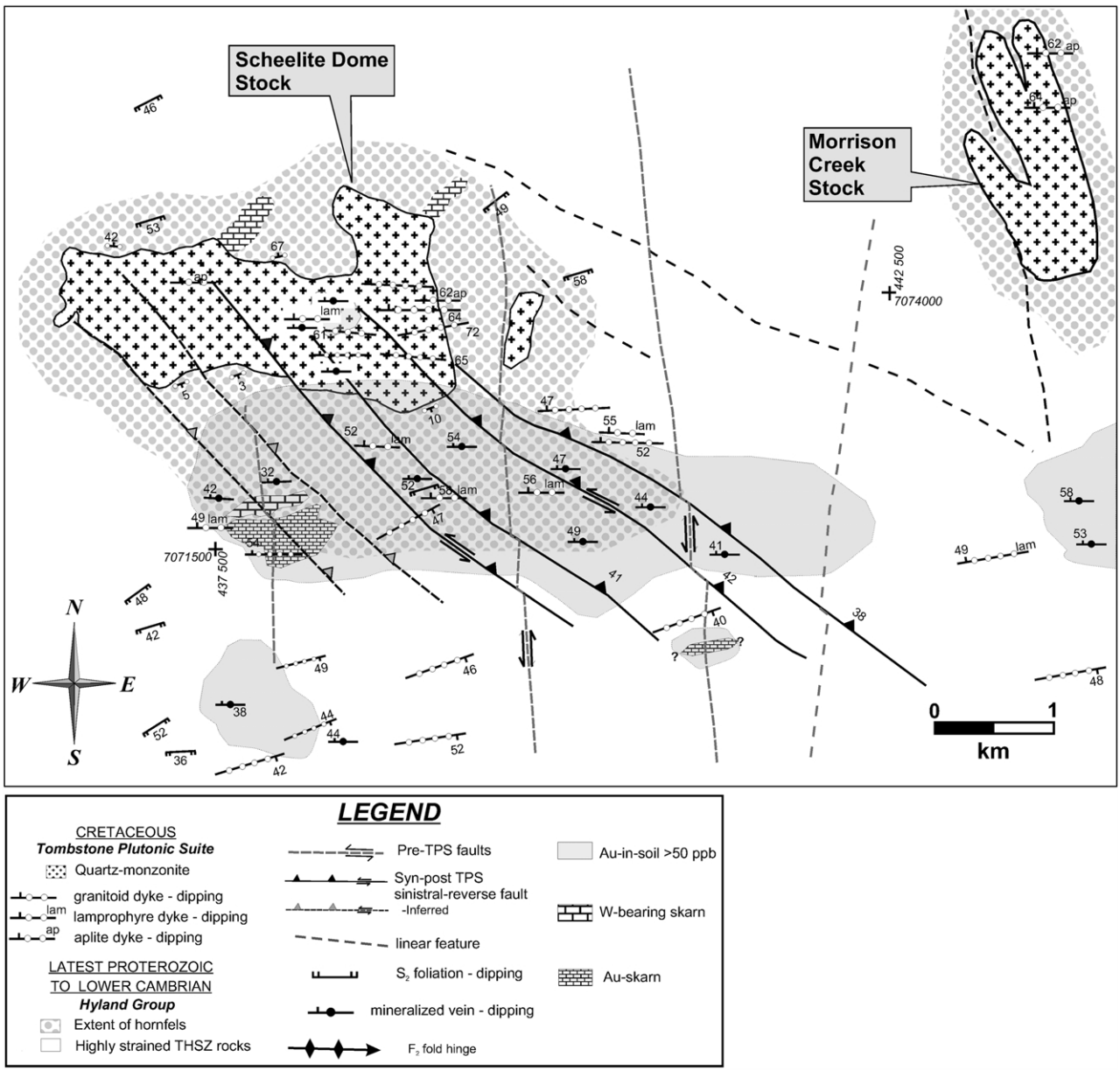

Fig. 5. Simplified geological map of the Scheelite Dome property showing the major gold mineralisation zones and structures. Auriferous veins are hosted in E-striking fractures and NW-striking faults. The apparent dextral offset along NW-striking sinistral-reverse faults across the stock's southern contact is a function of the gentle shallow dip of the contact.

E-striking, N-dipping extension fractures, to a lesser extent within NW-striking, NE-dipping faults and uncommonly along foliation planes (Hulstein et al., 1999; O'Dea et al., 2000; Fig. 3f and h). Sheeted extension vein arrays are best developed in relatively brittle host rocks such as quartzite, psammite and TPS intrusive rocks (Fig. 6a). Fault veins are restricted to more westerly-trending segments of NW-striking faults, and locally reach thicknesses in excess of 1 m. The fault veins are commonly brecciated and cemented by sulphide-rich assemblages (Fig. 6b). Fault veins and extension veins show mutually cross-cutting relationships, and thus are broadly coeval. N-striking subvertical faults do not host mineralised veins, but locally host barren buck quartz veins.

There are three main orientations of kilometre-scale faults and fractures present at Scheelite Dome: (1) N-striking, subvertical faults, (2) NW-striking, moderately NE-dipping, reverse-sinistral faults, and (3) WNW-striking, moderately N-dipping extension fracture zone broadly defined by the gold in soil anomaly (Hulstein et al., 1999; Mair et al., 2000; O'Dea et al., 2000; Fig. 3i). N-striking faults underwent sinistral offset prior to the emplacement of the TPS, with evidence for minor dextral reactivation following stock emplacement and related hydrothermal activity. In contrast, NW-striking faults clearly offset early

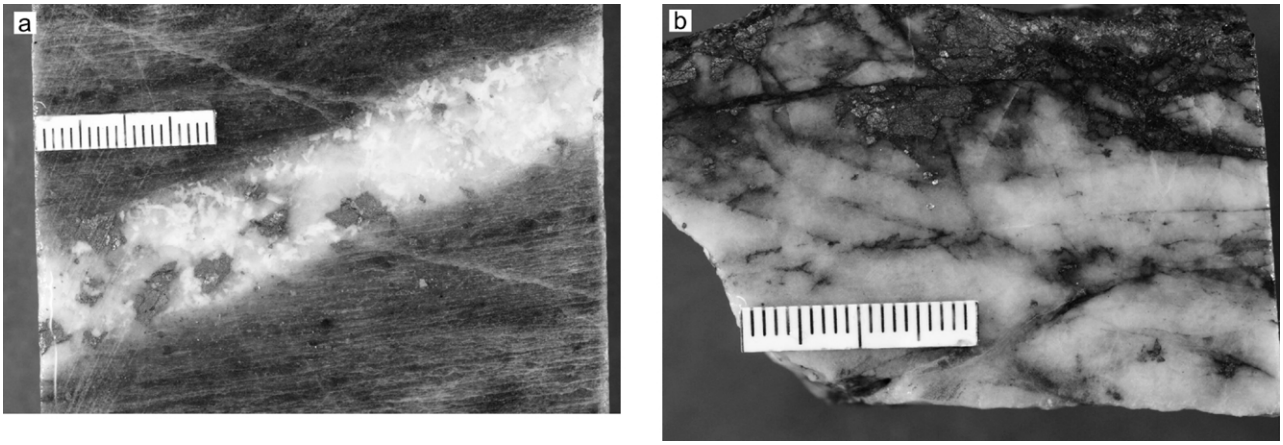

Fig. 6. (a) Sample of auriferous quartz–K-feldspar–arsenopyrite extension vein hosted in Hyland Group psammite at Scheelite Dome; scale bar is 4 cm long. (b) Sample of an auriferous fault vein showing multiple stages of cracking and sulphide deposition; scale bar is 4 cm long.

TPS intrusions, including the main Scheelite Dome stock (Fig. 5). Slickenlines on NW-striking fault surfaces plunge ~25° → 115°, and are about 70° to the intersection of NW-striking faults and E-striking extension veins (Fig. 3j). Offset lithological contacts and earlier developed fold hinges clearly indicate a reverse-sinistral movement sense. Notably, an apparent dextral displacement sense along NW-striking faults is indicated by the offset of the Scheelite Dome intrusion in plan view. This, however, is simply a function of the gentle SSE dip of the southern contact.

At Scheelite Dome the SSE-dipping foliation and N- to NNW-striking steep, early faults have had the most influence on stock emplacement. Dyke and sill emplacement was largely controlled by the existing foliation and E-striking fracture zones. Auriferous vein development was dominantly controlled by the E-striking fracture zones and NW-striking faults.

3.2.3. Dublin Gulch

The dominant foliation at Dublin Gulch strikes from NW to SW and has shallow to moderate dips, mostly with a westerly component (Templeman-Kluit, 1964). The Dublin Gulch stock, and associated smaller intrusions to the west, are elongate in an E- to ENE-direction. Shallow to moderate westerly dips of the contact of the main stock indicates a somewhat sill-like geometry largely controlled by the pre-existing foliation. Associated smaller granitoid intrusions occur in three main orientations: (1) steeply dipping E- to ENE-striking dykes, (2) sub-vertical NNW striking dykes, and (3) foliation parallel sills, commonly westerly dipping (Figs. 3l and 8a).

Sheeted, auriferous extension veins occur throughout the stock, with the highest densities and gold grades being in the Eagle and Olive Zones (Figs. 7 and 8b; Hitchens and Orssich 1995; Smit et al., 1996; Maloof et al., 2001). The Eagle Zone gold resource occurs in a comparatively laterally thin portion of the stock's cupola. The highest density of country rock-hosted sheeted veins is in the Shamrock Zone, adjacent to the NW contact of the stock (Fig. 7). The intrusion-hosted and country rock-hosted, auriferous, sheeted veins mostly strike ENE and are vertical to steeply S-dipping (Fig. 3m; Smit et al., 1996; Poulsen et al., 1997). A minor set of steeply east-dipping, N- to NNW-striking, sheeted veins occur exclusively in the hornfelsed country rocks. In metasedimentary rocks adjacent to the NW margin of the stock, gold occurs in E-striking segments of steeply dipping, ENE-striking, low displacement dextral faults that have dilational jogs with steep plunges (Fig. 8c–e).

Kilometre-scale fracture zones and low-displacement dextral faults on the property are steeply dipping and occur with a dominantly ENE strike, with a minor NE-striking subset (Fig. 3n). NW- to N-striking, steeply dipping faults/fractures also occur at Dublin Gulch and may have partially influenced emplacement of the stock.

4. Mechanical analysis

At the Clear Creek, Dublin Gulch and Scheelite Dome properties many of the granitoid stocks have NNW- (e.g. Saddle and Rhosgobel stocks, Clear Creek property; Fig. 2) or E-striking outcrop patterns (e.g. Scheelite Dome stock; Fig. 5). Stock contacts are mostly steep at Clear Creek, but at Scheelite Dome and Dublin Gulch they are both steep and largely concordant with the moderate to shallowly-dipping foliation. Dykes, sills and mineralised veins show four consistent orientations across the properties: (1) NNW- to N-striking, moderate- to steeply-dipping; (2) ~E-striking, steeply-dipping; (3) ENE-striking fault-veins; and (4) foliation concordant—dependant on local foliation orientation. The dominant set of broadly E-striking extension veins has also been reported widely from other deposits and prospects across the western Selwyn Basin (e.g. Brewery Creek; Poulsen et al., 1997; Lindsay and Baker, 2002).

The broadly E–W striking, sheeted auriferous veins show no displacement and mostly have unstrained quartz crystals aligned orthogonally to vein walls, and thus are

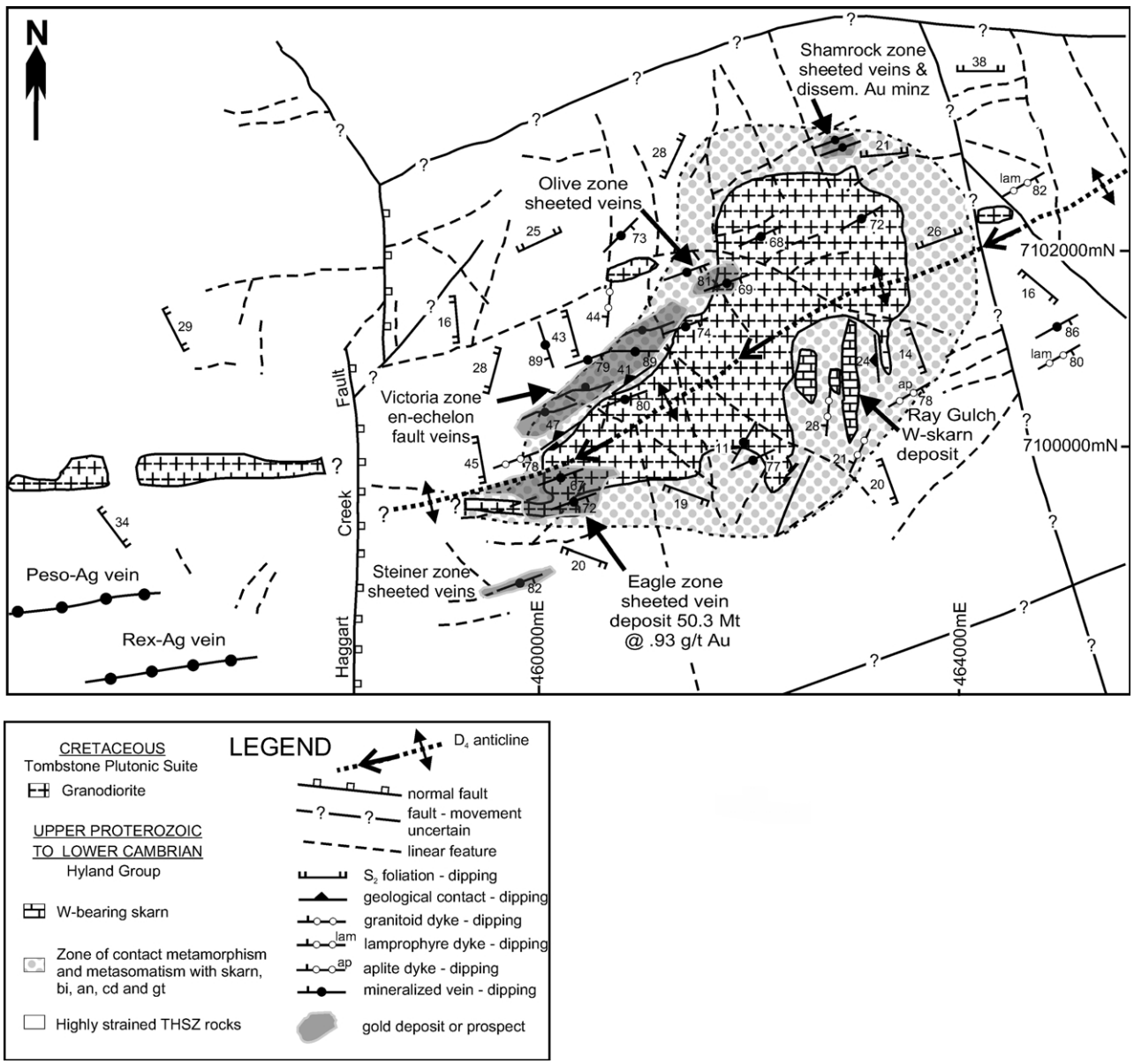

Fig. 7. Simplified geological map of the Dublin Gulch property showing the structural settings of the main zones of gold, base metal and tungsten mineralisation.

interpreted as extension veins. The tensile overpressure condition of fluid pressure exceeding the minimum principal stress ($P_f > \sigma_3$) must have been met for these to have formed (Sibson, 1992). The orientation of the extension veins and their internal quartz textures indicates the minimum principal stress, σ_3, was in a sub-horizontal, broadly N–S orientation. Thus the intermediate, σ_2, and maximum, σ_1, principal stresses would have been in a broadly E–W striking vertical plane (Fig. 9). Sinistral and sinistral-reverse slip on the NW–NNW striking faults and dextral movement on ENE striking structures are consistent with a sub-horizontal, E–W directed σ_1.

At all properties there is generally a lower abundance, and wider spacing of extension veins in the country rocks with respect to the granitoid stocks. There is, however, no deviation or deflection of extension vein orientations across granitoid-country rock contacts, indicating consistent orientation of the stress trajectories within and outside the stocks. Thus the emplacement and crystallisation of the stocks must have been essentially complete at the time of vein formation, with any stresses related to the intrusion having subsided. The differences between granitoid and country-rock properties were sufficient to affect extension vein density and abundance, but not orientation.

Tensile failure in the bulk rock resulted in formation of the E-striking extension veins, oriented parallel to σ_1 and orthogonal to σ_3, when the tensile overpressure condition was attained (Sibson, 1992). In this stress field the NW- to

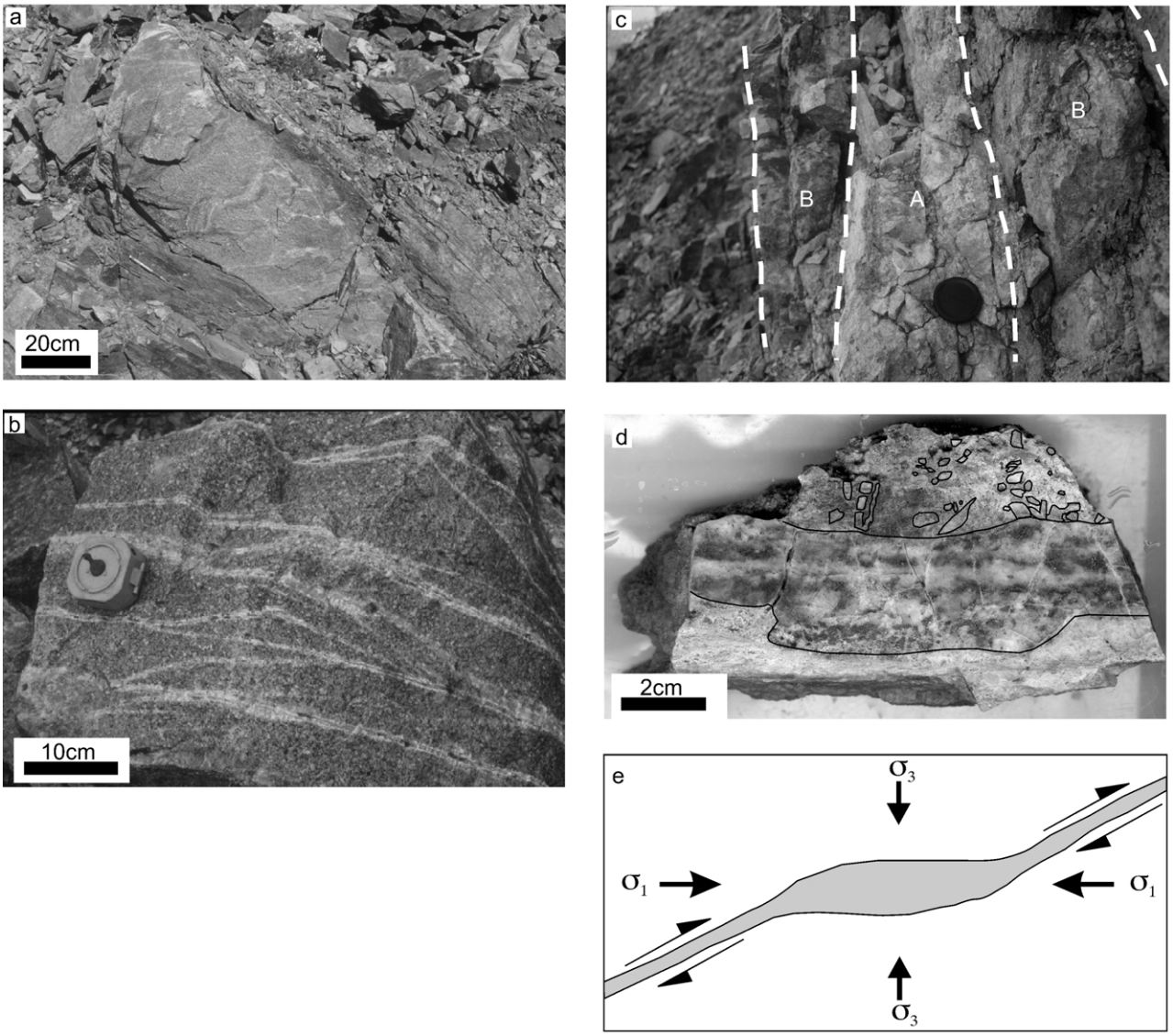

Fig. 8. (a) Photograph of a 30–40-cm-wide granodiorite dyke exploiting moderately W-dipping foliation near the NW contact of the Dublin Gulch stock; near-vertical face looking south. (b) Closely spaced, auriferous, sheeted quartz veins with K-feldspar selvages hosted in granodiorite at the Eagle Zone gold deposit, boulder not in place. (c) Vertical exposure, looking east of a 15–20-cm-wide quartz–arsenopyrite–gold vein (A) grading about 30 g/t Au, hosted in an E–W striking segment of a low displacement, steeply dipping, dextral fault in metapsammite in the Victoria Zone adjacent to the NW contact of the Dublin Gulch stock. Strongly sheared and sericite altered selvages (B) grade between 0.5 and 2 g/t Au. (d) Sample of fault vein from (c) with strongly brecciated and sericite/scorodite altered margins. (e) Schematic sketch in plan view of an auriferous dextral fault vein that forms part of the fault vein array of the Victoria Zone.

NNW-striking faults would have been misoriented, lying at 40–70° to σ_1 (Sibson, 1992; Fig. 9). Therefore these faults are likely to have developed pre- or early syn-magmatism, in a different stress field. Localised increases in fluid pressure associated with TPS intrusion-centred hydrothermal cells, may have caused refailure on these misoriented structures (e.g. Bear Paw breccia at Clear Creek and fault veins at Scheelite Dome). Mutually cross-cutting fault and extension veins indicate possible, localised fault-valve activity (Sibson, 1992).

Importantly, the arrays of E-striking extension veins could only have formed in the absence of through-going, cohesionless or low cohesion faults that were favourably oriented for failure (Sibson, 2001). In the inferred palaeostress field favourably oriented faults for reactivation would have been either ENE- (Fig. 9) or WNW-striking. Mineralised structures with an ENE strike occur at the Contact Zone on the Clear Creek property, and in particular the ENE-striking fault-veins of the Victoria Zone at Dublin Gulch (Figs. 2 and 7). Critically, however, these structures did not apparently develop into through-going faults, and thus probably allowed the continued formation of the E-striking extension fractures (cf. Sibson, 2001).

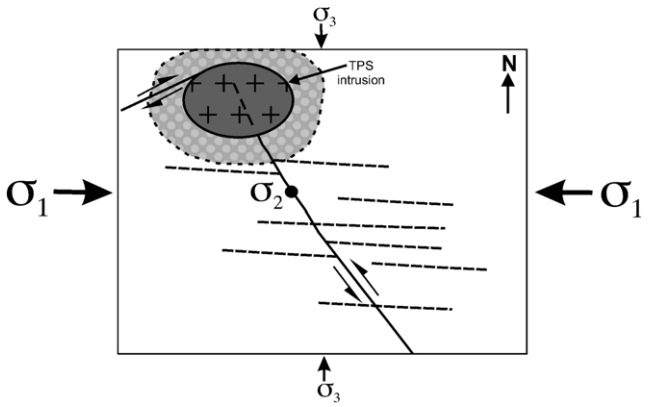

Fig. 9. Schematic sketch map illustrating the main mineralised structural elements and approximate likely principal stress axes operating over the Tombstone Gold Belt during the gold mineralisation stage.

5. Discussion

5.1. The regional stress field

The N- to NNW-striking, pre-TPS, dominantly strike-slip faults in the western Selwyn Basin are likely to have developed in a broadly N–S shortening regime. The fact that these faults cut THSZ fabrics indicates that they probably developed late-syn or post movement on the major Dawson, Tombstone and Robert Service thrusts in the Early Cretaceous. Sinistral reactivation of the NW- to NNW-striking faults occurred in association with TPS magmatism and hydrothermal activity at ~92 Ma.

The presence of a mineralisation-controlling normal fault and associated steeply-dipping, E-striking extension veins at the Brewery Creek mine, which was at a higher structural level than the three deposits in this study, indicates that σ_1 there was oriented vertically (Lindsay and Baker, 2002). Thus, at ~92 Ma, σ_1 was sub-horizontal to moderately plunging at Clear Creek, Scheelite Dome and Dublin Gulch, but sub-vertical at Brewery Creek. One possible explanation for this is that σ_1 and σ_2 were close to equal in magnitude, thus easily allowing interchange of the σ_1 orientation.

Reconciling the formation of the E-striking extension fractures in the western Selwyn basin with the plate vectors in the mid-Cretaceous is difficult. At ca. 100 Ma there was NE-directed convergence of the Farallon plate with the North American Craton (Plafker and Berg, 1994). A period of crustal extension between 130 and 110 Ma in the adjacent Yukon–Tanana Terrane has been proposed by Pavlis (1989) and Miller and Hudson (1994). Shallowly dipping Jura–Cretaceous fabrics, extension lineations and kinematic indicators of the THSZ appear to correlate with this extensional event. The N–S-trending σ_3 and E–W-directed, horizontal σ_1 determined from this study therefore do not directly reflect the NE convergence of the Farallon plate, or the NW–SE extensional event between 130 and 110 Ma. It may be that the ~92 Ma mineralised structures of the TGB represent a transitional stress-regime between the waning stages of the 130–110 Ma extensional event and initiation of major movement on the Tintina Fault at ~70 Ma in response to northward translation of the Pacific Plates (Engebretson et al., 1985; Goldfarb et al., 2000).

5.2. Structural comparisons to other epigenetic deposit types

TGB deposits are similar to porphyry style gold systems, and polymetallic intrusion-related systems, such as those of the Cornubian Batholith, SW England, in that mineralisation has a close spatial and temporal relationship to intrusions. However, porphyry systems commonly have variably-oriented stockworks and/or breccias at their centres. In both porphyry and polymetallic intrusion-related systems concentric and radial vein arrays are common, and reflect magmatic processes (Tosdal and Richards, 2001). Planar vein arrays also occur, but in general are more prevalent outside the area of influence of intrusive centres (e.g. Moore, 1975; Heidrick and Titley, 1982) and at deeper crustal levels in some deposits (Tosdal and Richards, 2001). Although the polymetallic deposits of the Cornubian ore field show a strong regional structural control, they are dominated by structures of highly variable orientation close to their hydrothermal centres (Moore, 1975).

The critical difference in structural style of the TGB deposits to porphyry and Cornubian-style systems is that there are regionally consistent vein and fault orientations both within and outside areas of influence of the TPS intrusions and their hydrothermal centres. We propose that one of the major reasons for these differences is that most TGB deposits were formed at depths between 3 and 7 km (Baker and Lang, 1999; Marsh et al., 2003), deeper than most porphyry and Cornubian-style systems (Moore, 1975; Tosdal and Richards, 2001). In general, mean and differential stress will increase with depth, and consequently a single fracture orientation is favoured in the TGB. In shallower environments, however, mean and differential stresses may be lower, allowing stresses associated with intrusion emplacement to dominate the local stress field.

Hydrothermal gold deposits formed in the upper crust show a wide range of structural and veining styles. The different structural styles are mainly a result of the various failure modes induced by stress states and degree of fluid overpressuring required for vein formation. The failure modes in bulk rock are: compressional shear when the differential stress, $\Delta\sigma > 5.66T$ (where T = bulk rock tensile strength), hybrid extensional shear when $4T < \Delta\sigma < 5.66T$ and purely extensional failure when $\Delta\sigma < 4T$ (Fig. 10a; Sibson, 1998). These failure modes provide appropriate reference conditions to describe styles of epigenetic, structurally-controlled gold deposits.

Planar extension vein arrays and mineralised, compressional strike-slip faults (e.g. Bear Paw breccia and Scheelite Dome) dominate deposits of the TGB. Other mineralisation styles include hybrid extensional shear veins (e.g. Victoria

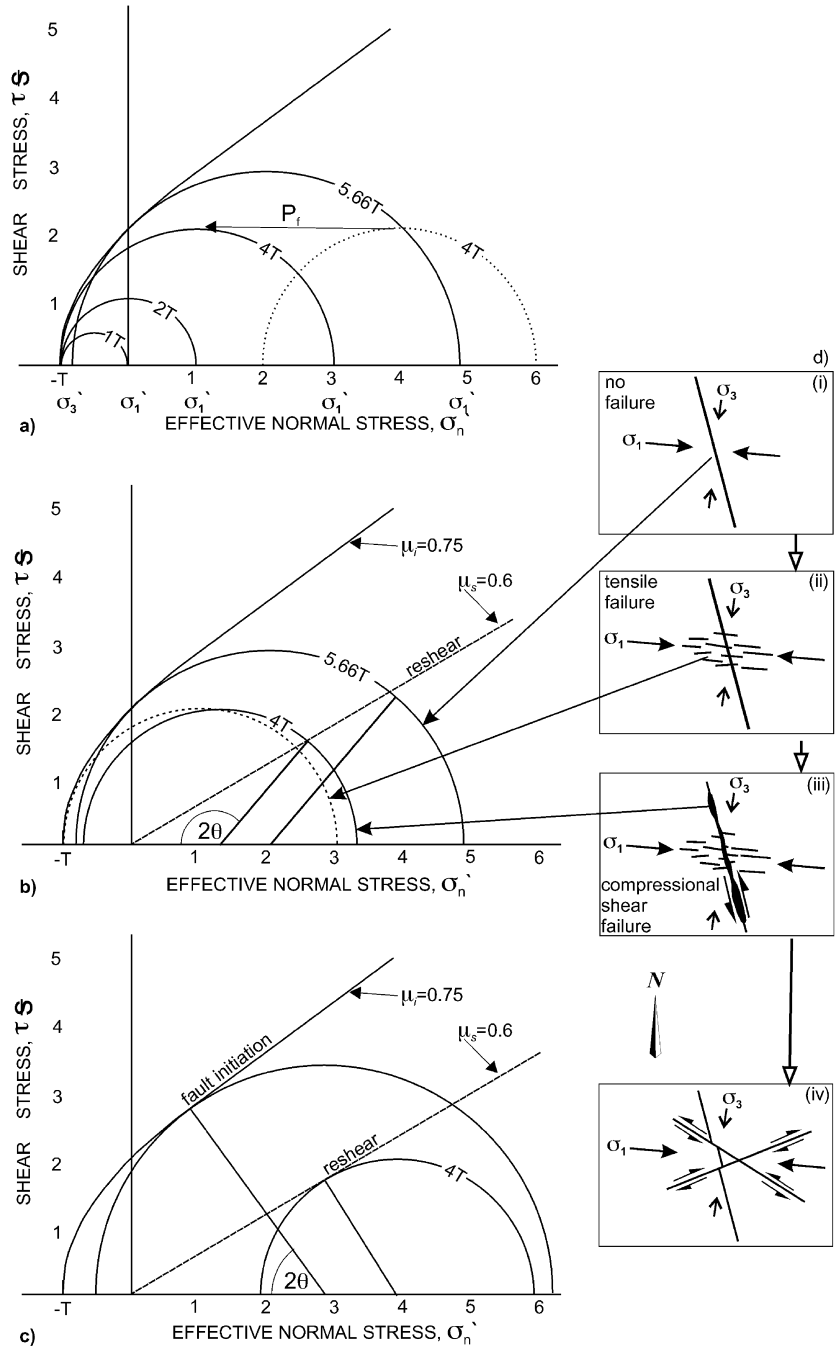

Fig. 10. (a) Generic Mohr diagram with a composite Griffith–Coulomb failure envelope for intact rock normalised to tensile strength, T, with a coefficient of internal friction, $\mu_i = 0.75$ in the compressional field (modified from Sibson, 1998). The critical stress circles shown represent boundary conditions for the various modes of failure in bulk rock. Where $\Delta\sigma > 5.66T$ compressional shear failure (faults) will result. Where $4T < \Delta\sigma < 5.66T$ hybrid extensional-shear failure will occur. Where $\Delta\sigma < 4T$ pure extensional failure will occur with fractures developing orthogonally to σ_3. Where $\Delta\sigma$ becomes closer to zero (e.g. 1 or $2T$) the likelihood of multiple vein orientations increases (see text). (b) Mohr diagram showing reshear criteria for existing, severely misoriented faults where $\theta = 65°$ and the static friction coefficient for reshear, $\mu_s = 0.6$ (Sibson, 1998). Where $\Delta\sigma = 4T$ reshear will occur on the severely misoriented fault. However, a small increase in the θ angle may result in bulk rock failure, as represented by the dashed circle (pure extensional or hybrid-extensional shear). Where $\Delta\sigma = 5.66T$ and $\theta = 65°$ refailure will not occur on the existing fault. Instead the bulk rock can fail in hybrid-extensional or compressional shear mode. However, a small reduction in μ_s, represented by the dotted line, will result in refailure on the existing, severely misoriented faults. (c) Mohr diagram showing criteria for formation and reshear of optimally oriented cohesionless faults. For the example where $\Delta\sigma > 5.66T$ faults will generally form at a θ angle of $\sim 27°$ when $\mu_s = 0.75$. When existing, optimally oriented faults for reshear are present they will fail at much lower differential stresses and higher effective normal stresses (lower pore pressures). (d) Sketches showing structural relationships and likely principal stress axes (specific angles from Clear Creek) with respect to failure criteria represented in (b) and (c). (i) NNW-striking, pre-existing, severely misoriented faults are locked up. (ii) With increasing pore pressure and a low differential stress, $\Delta\sigma < 4T$, extensional 1D failure occurs in the bulk rock sequentially with (iii) failure on pre-existing, misoriented faults. (iv) Initiation or reshear on cohesionless, favourably oriented, ENE and/or WNW striking faults would not allow the extension fractures to form, or could end the period of formation of extension fractures.

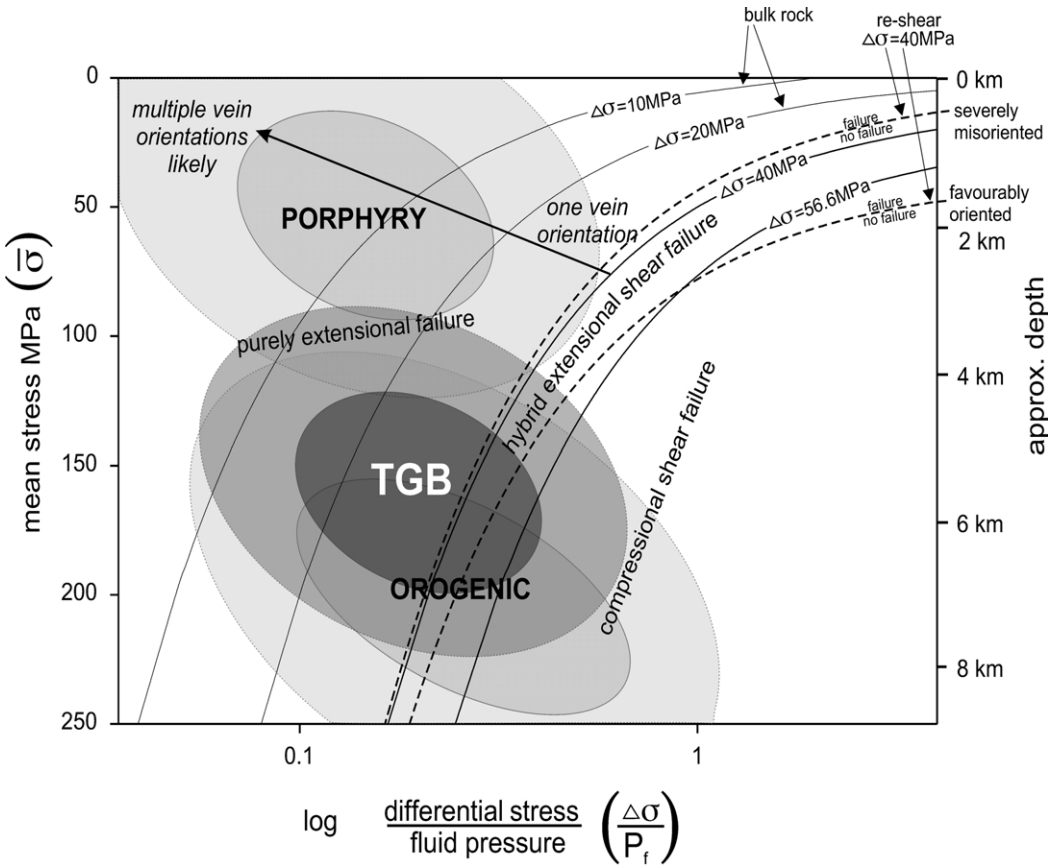

Fig. 11. Diagrammatic representation of the ratio of differential stress to fluid pressure required for failure plotted against mean stress as a proxy for depth (assuming constant rock density), with inferred fields of interest for the indicated deposit styles. The fields for the different failure modes in bulk rock were plotted using a rock tensile strength of $T = 10$ MPa and differential stress values of 1, 2, 4 and 5.66T (solid lines). The arrow represents a decreasing $\Delta\sigma$ and thus an increasing likelihood of multiple vein orientations, because repetitive change of principal stress orientations is likely at very small differential stresses (Tosdal and Richards, 2001). The dotted lines represent reshear on a severely misoriented fault ($\theta = 65°$) and reshear on an optimally oriented ($\theta \sim 29.5°$) existing fault with a coefficient of static friction for reshear of $\mu_s = 0.6$ (Sibson, 1998) when the $\Delta\sigma = 4T$ (cf. Fig. 10). Note that the curve for refailure on this misoriented fault closely approximates the extension (sheeted veins) failure mode for $4T$ (solid line; cf. Fig. 10). From Fig. 10 it can be seen that very small changes in fault orientation, differential stress and the coefficient of static friction for reshear will affect the failure mode, and therefore the structural style of the ore deposit. The diagram emphasises how the interplay of differential stress and fluid pressure influences the failure mode and thus ore deposit styles at various depths in the upper crust.

Zone at Dublin Gulch) and hydrothermal breccias (Bear Paw breccia). The dominance of extension veins suggests a relatively low differential stress magnitude of $<4T$, assuming average rock properties of Sibson (1998) (Fig. 10a and b). Failure on misoriented faults and sequential development of sheeted veins is therefore possible at these relatively low differential stress values (Fig. 10b). Formation of, or refailure on optimally oriented, cohesionless faults or low cohesion faults, if present, would prevent failure in bulk rock or on pre-existing misoriented faults, potentially preventing, or terminating formation of these mineralised systems (Sibson, 2001; Fig. 10c).

Refailure and fluid-driven fault-valving has been inferred as a mechanism for the formation of many orogenic deposits (e.g. Robert and Brown, 1986; Sibson, 1992; Cox et al., 2001). The overall geometry of the strike-slip fault-veins and extension veins in TGB deposits is similar (although turned sideways) to that for steep reverse faults with associated horizontal extension veins in orogenic gold systems (Robert and Brown, 1986; Sibson, 1992). The first critical difference we infer is that failure on misoriented NW- to NNW-striking faults in the TGB would have only occurred in localised areas where fluid released from TPS-related hydrothermal cells could cause fluid overpressuring. Fluid pressure cycling would be small in amplitude compared with a reverse fault system at the same depth (Sibson, 1992).

5.3. Stress and pore pressure constraints on failure modes

For any given depth in the upper crust the failure mode is controlled by the interplay of the stress state and pore pressure, P_f, so that diverse failure modes are possible However, increasing mean stress (depth) requires greater pore pressures to induce brittle failure for a given $\Delta\sigma$. The most commonly observed failure modes differ significantly for the major types of epigenetic, vein-hosted mineralisation (Fig. 11).

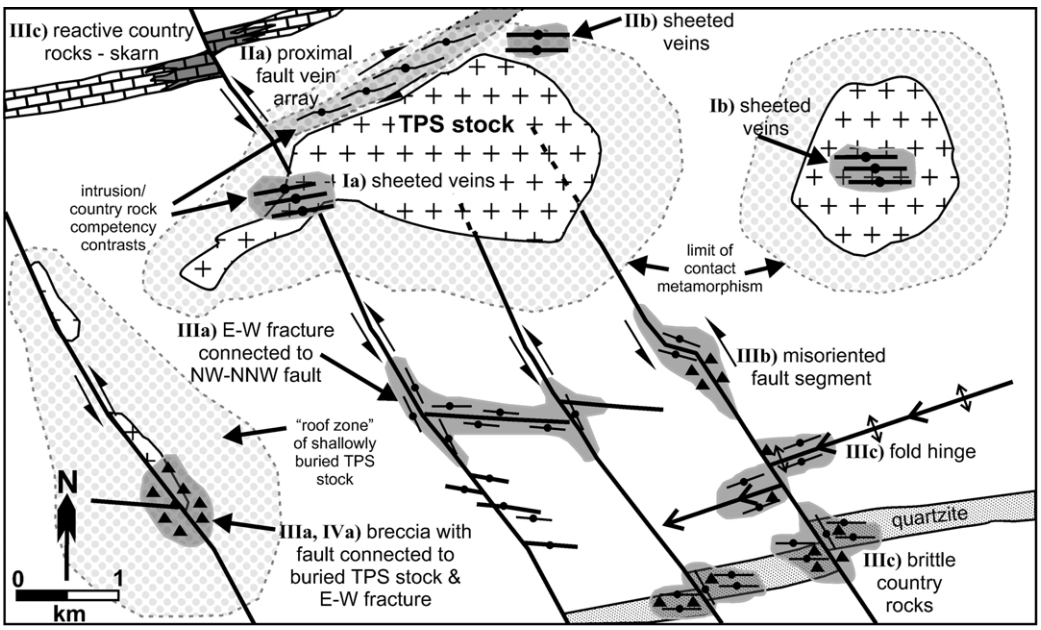

Fig. 12. Structural exploration model for intrusion-related gold deposits in the TGB depicting favourable structural sites (heavy shading) for mineralisation (incorporating ideas from Hart et al. (2000) and Lang et al. (2000)). Favourable structural sites include broadly E-striking sheeted veins hosted in intrusions: (Ia) thinned zones of stocks (e.g. Eagle Zone deposit at Dublin Gulch) and (Ib) in cupolas of TPS stocks (e.g. Eagle Zone at Dublin Gulch, Rhosgobel/Pukelman/Eiger stocks at Clear Creek). Proximal fault-veins in contact aureoles: (IIa) adjacent to stock contacts (e.g. Victoria Zone at Dublin Gulch, Contact Zone at Clear Creek) and (IIb) E-striking fracture zones adjacent to, or above a TPS stock (e.g. Steiner and Shamrock Zones at Dublin Gulch). Distal veins and breccias with structures linked to TPS stocks: (IIIa) at the intersection of NNW- to NW-striking faults and E-striking fracture zones (e.g. Scheelite Dome, Bear Paw breccia at Clear Creek); (IIIb) westerly-misoriented sections of NNW- to NW-striking faults, creating dilational jog geometries (e.g. Scheelite Dome) and (IIIc) at the intersection of NNW- to NW-striking faults or E-striking fracture zones and earlier developed fold hinges, competent units such as quartzite or chemically reactive calcareous rocks (e.g. Scheelite Dome—competent quartzite unit and skarn). (IVa) NNW- to NW-striking fault connected vertically to a buried TPS stock.

Delaney et al. (1986) defined the driving stress ratio that was used to illustrate the role of pore fluid pressure (P_f), mean stress (σ_m), differential stress ($\Delta\sigma$) and the angle between σ_1 and the fracture orientation (θ) in the opening of pre-existing fractures. A useful graphical modification of this relationship plots the ratio (r) of differential stress to pore pressure (P_f) required for failure in bulk rock and along pre-existing fractures or faults (Eq. (1); Fig. 11). This diagram therefore portrays the different degrees of fluid overpressuring required for various failure modes relative to depth (as a proxy for mean stress, σ_m). Specific curves were calculated trigonometrically from Mohr diagrams (Fig. 10) for the critical $\Delta\sigma$ values of 4 and 5.66T, which represent boundary conditions for different failure modes in bulk rock with average properties (Sibson, 1998; Fig. 10a). For example, for the critical circle representing boundary conditions between extensional shear failure and purely extensional failure (where $\Delta\sigma = 4T$) in bulk rock with $T = 10$ MPa, then;

$$r = \frac{\Delta\sigma}{\sigma_m - T} = \frac{40\text{MPa}}{\sigma_m - 10\text{MPa}} \quad (1)$$

The refailure conditions for a severely misoriented ($\theta = 65°$) fault (cf. Fig. 10b) are very close to those for purely extensional failure in bulk rock (Fig. 11). This illustrates the common structural feature in many orogenic, and some TGB deposits of episodic refailure on misoriented faults and sequential development of extension veins. Thus in the TGB the stress and fluid pressure conditions required for failure on the extension fractures and misoriented faults would have been very similar (Fig. 10b). Pre-existing, optimally oriented ($\theta \sim 27°$) faults, if present, would have failed preferentially over misoriented faults, at lower fluid pressures (Fig. 11; cf. Fig. 10c).

Approximate fields for porphyry, TGB and orogenic gold deposits with respect to their major modes of failure, stress state and pore pressure conditions are shown in Fig. 11. Porphyry deposits generally have the largest variation in vein orientations, with concentric, radial and orthogonal veins, and stockworks and breccias common. The multiple vein orientations commonly observed in porphyry systems are likely because of small differential stresses, allowing repeated exchange of principal stress orientations (Tosdal and Richards, 2001; Fig. 11). Tombstone Gold Belt deposits are dominated by planar extension vein arrays, with lesser hybrid extensional shear veins (e.g. Victoria Zone at Dublin Gulch), stockworks (e.g. Saddle Stock at Clear Creek) and hydrothermal breccias (e.g. Bear Paw breccia at Clear Creek). Orogenic deposits have a wide range of mineralisation styles, but are generally dominated by compressional shear veins, hybrid extensional shear veins and extension

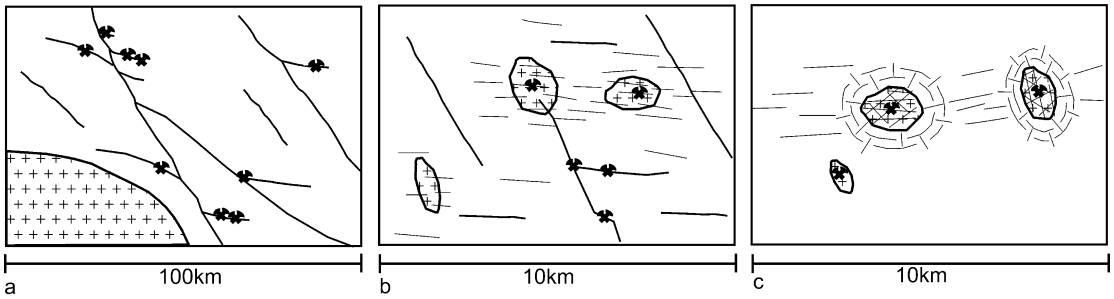

Fig. 13. Schematic sketches illustrating the importance of structural linking in orogenic, TGB and porphyry gold systems. (a) Orogenic gold deposits generally are structurally linked to regional-scale faults or shear zones. (b) In the TGB NNW- to NW-striking faults and E-striking fracture zones are regionally extensive, but are not connected to any regional-scale faults or shear zones, and are only mineralised in the presence of TPS intrusions. (c) Porphyry systems generally have more variable vein orientations, with most deposits centred near intrusion cupolas.

veins with more rare stockwork and breccia zones. We infer that this variation in behaviour is a consequence of the effect of increasing depth on influencing the variety of failure modes. Steep reverse faults in compressional environments, such as those associated with many orogenic systems, require the highest level of fluid overpressuring for failure and void formation (e.g. Sibson, 1992; Robert et al., 1995). Strike-slip faults associated with TGB deposits and in parts of some orogenic systems (e.g. some of those in the Yilgarn Craton, Western Australia; Groves et al., 1998) require intermediate levels of overpressuring for failure. High-level porphyry and epithermal systems require the lowest levels of fluid overpressuring for vein formation, and extension fractures can form under hydrostatic fluid pressures in a potentially wide range of orientations (Tosdal and Richards, 2001).

6. Implications for exploration

Recent studies in complex brittle settings demonstrate that major mineralised hydrothermal systems develop where fracture/fault/shear systems link up and develop sufficient connectivity to create networks that link fluid source rocks to favourable sites for ore deposition (e.g. Jiang et al., 1997; Cox, 1999). Relatively well-connected faults may form long-distance fluid channelways and ore deposition may occur at specific structural sites such as terminal fault branches, faults in particular orientations, and smaller faults that connect larger faults.

In the TGB, E-striking extensional fracture zones connected to the NW- to NNW-striking faults are favourable sites for enhanced permeability and thus gold mineralisation (Fig. 12). Scheelite Dome is a good example of this fault/fracture geometry, where NW-striking, mineralised faults are connected to E-striking, extensional veins (Fig. 5). The Bear Paw breccia zone at Clear Creek occurs along a NNW-striking fault (Fig. 2). It likely overlies a larger intrusion at depth, as indicated by contact metamorphic assemblages and EM survey data, and suggests mineralising fluids may have been channelled vertically up the fault. Other prospective fault/fracture geometries include more westerly-misoriented segments of NW- to NNW-striking faults or smaller, near E-striking fracture zones that may link two larger NW- to NNW-striking faults (Fig. 12).

The type of potential deposit, and hence exploration target, is influenced by the degree of structural interconnectivity, particularly the extent to which structural channels may have linked into TPS stock-centred hydrothermal cells. The stocks may have become partially sealed by hornfelsing of the surrounding host rocks and in this case over-pressuring may have occurred within the stock, with sheeted vein-style, intrusion-hosted mineralisation resulting. If, however, the hornfels seals were breached by faults, fluids could potentially be channelled into an area with a suitable structural geometry for focusing, potentially resulting in the formation of a country-rock hosted gold deposit.

Finally, a common feature of orogenic gold districts is the structural linking of the deposits to regional-scale faults or shear zones (Fig. 13a; Groves et al., 1998; Cox et al., 2001). Porphyry systems generally have less systematic regional consistency in vein orientations, with most mineralisation centred on intrusion cupolas (Fig. 13c). In the TGB, however, mineralisation controlling NNW- to NW-striking faults and E-striking fractures are regionally extensive but are not linked to any regional-scale (>5 km length) faults or shear zones, and are mineralised only in the presence of TPS-related hydrothermal cells (Fig. 13b). The TGB gold mineralisation therefore provides a useful bridge in understanding the diversity of mechanically controlled structural styles in otherwise mostly unrelated deposit types.

Acknowledgements

We acknowledge the Yukon Geology Program/James Cook University collaborative grant for logistical and financial support. The SEG Student Grant Scheme and the USGS provided additional analytical and financial support.

Reviews by Richard Sibson and Howard Poulsen helped to improve the manuscript and are appreciated. In particular, detailed comments by R. Sibson on the mechanical analysis stimulated a more rigorous attempt to define the role of depth versus failure mode for different deposit types. Rich Goldfarb is acknowledged for comments that helped vastly improve the manuscript. We would like to acknowledge field support from the Yukon Geology Program, the Harper family of Blackstone Placer Mining, Redstar Resources, Mike Stammers, Ted Takacs, Veronica Brown, Laurie Cortesi, Erin Marsh and Mark Lindsay.

References

Baker, T., Lang, J.R., 1999. Geochemistry of hydrothermal fluids associated with intrusion hosted gold mineralization, Yukon Territory. In: Stanley, C.J., et al. (Eds.), Mineral Deposits: Processes to Processing, Balkema, Rotterdam, pp. 17–20.

Bakke, A., 1995. The Fort Knox "porphyry" gold deposit: structurally controlled stockwork and shear quartz vein, sulfide poor mineralization hosted by a Late Cretaceous pluton, east-central Alaska. In: Schroeter, T.G. (Ed.), Porphyry Deposits of the Northwestern Cordillera of North America. Canadian Institute of Mining and Metallurgy, Special Volume 46, pp. 795–802.

Coombes, S., 1996. 1995 Exploration report on the Clear Creek option (text and maps). Kennecott Canada Inc.

Cox, S.F., 1999. Deformational controls on the dynamics of fluid flow in mesothermal gold systems. In: McCaffrey, K.J.W., Lonergan, L., Wilkinson, J.J. (Eds.), Fractures, Fluid Flow and Mineralization. Geological Society, London, Special Publications 155, pp. 123–140.

Cox, S.F., Knackstedt, M.A., Braun, J., 2001. Principles of structural control on permeability and fluid flow in hydrothermal systems. Society of Economic Geologists Reviews 14, 1–24.

Delaney, P.T., Pollard, D.D., Ziony, J.I., McKee, E.H., 1986. Field relations between dikes and joints: emplacement processes and paleostress analysis. Journal of Geophysical Research 91 (B5), 4920–4938.

Diment, R., Craig, S., 1999. Brewery Creek gold deposit, central Yukon. In: Roots, C.F., Emond, D.S. (Eds.), Yukon Exploration and Geology 1998, Exploration and Geological Services Division, Yukon, Indian and Northern Affairs, Canada, pp. 225–230.

Ebert, S., Miller, L., Petsel, S., Dodd, S., Kowalczyk, P., 2000. Geology, mineralization, and exploration at the Donlin Creek Project, southwestern Alaska. In: The Tintina Gold Belt: Concepts, Exploration, and Discoveries. British Columbia and Yukon Chamber of Mines, Vancouver, Canada, Special Volume 2, pp. 99–114.

Engebretson, D.C., Cox, A., Gordon, R.G., 1985. Relative motions between oceanic and continental plates in the Pacific Basin. Geological Society of America Special Paper 206.

Gabrielse, H., Yorath, C.J., 1991. Tectonic synthesis. In: Gabrielse, H., Yorath C.J. (Eds.), Geology of the Cordilleran Orogen in Canada. Geological Survey of Canada, Geology of Canada 4, pp. 677–705, Chapter 18.

Goldfarb, R., Hart, C., Miller, M., Farmer, G.L., Groves, D., 2000. The Tintina Gold Belt—a global perspective. In: The Tintina Gold Belt: Concepts, Exploration and Discoveries. British Columbia and Yukon Chamber of Mines Special Volume 2, pp. 5–34.

Gordey, S.P., Anderson, R.G., 1993. Evolution of the northern Cordilleran miogeocline, Nahanni map area (105I), Yukon and Northwest Territories. Geological Survey of Canada Memoir 428.

Groves, D.I., Goldfarb, R.J., Gebre-Mariam, M., Hagemann, S.G., Robert, F., 1998. Orogenic gold deposits: a proposed classification in the context of their crustal distribution and relationship to other gold deposit types. Ore Geology Reviews 13, 7–27.

Hart, C.J.R., Baker, T., Burke, M., 2000. New exploration concepts for country-rock-hosted, intrusion-related gold systems, Tintina Gold Belt in Yukon. In: Jambor, J.L. (Ed.), The Tintina Gold Belt: Concepts, Exploration and Discoveries. British Columbia and Yukon Chamber of Mines Special Volume 2, pp. 45–172.

Hart, C.J.R., McCoy, D.T., Goldfarb, R.J., Smith, M., Roberts, P., Hultstein, R., Bakke, A.A., Bundtzen, T.K., 2002. Geology, exploration, and discovery in the Tintina Gold Province, Alaska and Yukon. Society of Economic Geologists Special Publication 9, 241–274.

Heidrick, T.L., Titley, S.R., 1982. Fracture and dike patterns in Laramide plutons and their structural and tectonic implications: American southwest. In: Titley, S.R., (Ed.), Advances in Geology of the Porphyry Copper Deposits, University of Arizona Press, pp. 73–91.

Hitchens, A.C., Orssich C.N., 1995. The Eagle zone gold–tungsten sheeted vein porphyry deposit and related mineralization, Dublin Gulch, Yukon Territory. In: Schroeter, T.G. (Ed.), Porphyry Deposits of the Northwestern Cordillera of North America. Canadian Institute of Minerals and Metallogeny, Special Volume 37, pp. 245–254.

Hulstein, R., Zuran, R., Carlson, G.G., Fields, M., 1999. The Scheelite Dome gold project, central Yukon. In: Emond, D.S., Weston, L. (Eds.), Yukon Exploration and Geology 1999, Exploration and Geological Services Division, Yukon, Indian and Northern Affairs, Canada, pp. 243–253.

Jiang, Z., Oliver, N.H.S., Barr, T.D., Power, W.L., Ord, A., 1997. Numerical modeling of fault-controlled fluid flow in the genesis of tin deposits of the Malage Ore Field, Gejiu Mining District, China. Economic Geology 92, 228–247.

Lang, R.L., Baker, T., Hart, C.J.R, Mortensen, J.K., 2000. An exploration model for intrusion-related gold systems. Society of Economic Geologists Newsletter 40.

Lennan, W.B., 1983. Ray Gulch tungsten skarn deposit, Dublin Gulch area, central Yukon. In: Morin, J.A. (Ed.), The Canadian Institute of Mining and Metallurgy, Special Volume 37, pp. 245–254.

Lindsay, M.J., Baker, T., 2002. Brittle structural controls on the distribution of gold mineralization in an intrusion-related gold deposit, Brewery Creek mine, Yukon, Canada. In: McLellan, J., Brown, M. (Eds.), Deformation, Fluid Flow and Mineralization (Rick Sibson Symposium), EGRU Special Publication 60, pp. 87–94.

Mair, J.L., Hart, C.J.R., Goldfarb, R.J., O'Dea, M., Harris, S., 2000. Geology and metallogenic signature of gold occurrences at Scheelite Dome, Tombstone Gold Belt, Yukon Territory. In: Emond, D.S., Weston, L. (Eds.), Yukon Exploration and Geology 1999, Exploration and Geological Services Division, Yukon, Indian and Northern Affairs, Canada, pp. 165–176.

Maloof, T.L., Baker, T., Thompson, J.F.H., 2001. The Dublin Gulch intrusion-hosted gold deposit, Tombstone plutonic suite, Yukon Territory, Canada. Mineralium Deposita 36, 583–593.

Marsh, E.E., Hart, C.J.R., Goldfarb, R.J., Allen, T.L., 1999. Geology and geochemistry of the Clear Creek gold occurrences, Tombstone gold belt, central Yukon Territory. In: Roots, C.F., Emond, D.S. (Eds.), Yukon Exploration and Geology 1998, Exploration and Geological Services Division, Yukon, Indian and Northern Affairs, Canada, pp. 185–196.

Marsh, E.E., Goldfarb, R.J., Hart, C.J.R., Johnson, C., 2003. Geology and geochemistry of the Clear Creek intrusion-related gold occurrences, Tintina Gold Belt, Yukon, Canada. Canadian Journal of Earth Sciences 40, 681–699.

McCoy, D., Newberry, R.J., Layer, P., DiMarchi, J.J., Bakke, A., Masterman, S., Minehane, D.L., 1997. Plutonic-related gold deposits of Interior Alaska, In: Goldfarb, R.J., Miller, L.D. (Eds.), Economic Geology Monograph 9, pp. 191–241.

Miller, E.L., Hudson, T.L., 1994. Mid-Cretaceous extensional fragmentation of a Jurassic–Early Cretaceous compressional orogen, Alaska. Tectonics 10 (4), 781–796.

Moore, M., 1975. A mechanical interpretation of the vein and dyke systems of the SW England orefield. Mineralium Deposita 10, 374–388.

Mortensen, J.K., Hart, C.J.R., Murphy, D.C., Heffernan, S., 2000. Temporal

evolution of Early and mid-Cretaceous magmatism in the Tintina Gold Belt. In: The Tintina Gold Belt: Concepts, Exploration and Discoveries. British Columbia and Yukon Chamber of Mines, Special Volume 2, pp. 49–57.

Murphy, D.C., 1997. Geology of the McQuesten River region, northern McQuesten and Mayo map areas, Yukon Territory (115P/14, 15, 16; 105M/13, 14). Exploration and Geological Services Division, Yukon, Indian and Northern Affairs Canada, Bulletin 6.

Murphy, D.C., Héon, D., 1994. Geological overview of Sprague Creek map area, westeren Selwyn Basin. In: Editor, X., (Ed.), Yukon Exploration and Geology 1994, Exploration and Geological Services Division, Yukon, Indian and Northern Affairs, Canada, pp. 29–46.

O'Dea, M., Carlson, G., Harris, S., Fields, M., 2000. Structural and metallogenic framework for the Scheelite Dome deposit, Yukon Territory. In: The Tintina Gold Belt: Concepts, Exploration and Discoveries. British Columbia and Yukon Chamber of Mines, Special Volume 2, pp. 115–129.

Pavlis, T.L., 1989. Middle Cretaceous orogenesis in the northern Cordillera; a Mediterranean analog of collision-related extensional tectonics. Geology 17, 947–950.

Plafker, G., Berg, H.C., 1994. Overview of the geology and tectonic evolution of Alaska. In: Plafker, G., Berg, H.C. (Eds.), The Geology of Alaska: The Geology of North America, G-1, Geological Society of America, Boulder, Colorado, pp. 989–1021.

Poulsen, K.H., Mortensen, J.K., Murphy, D.C., 1997. Styles of intrusion related gold mineralization in the Dawson–Mayo area, Yukon. Current Research, Geological Survey of Canada 1997, 1–11.

Robert, F., Brown, A.C., 1986. Archaean gold-bearing quartz veins at the Sigma mine, Abitibi greenstone belt, Quebec: Part I—Geologic relations and formation of the vein system. Economic Geology 81, 578–592.

Robert, F., Boullier, A.M., Fidaous, K., 1995. Gold–quartz veins in metamorphic terranes and their bearing on the role of fluids in faulting. Journal of Geophysical Research 100, 12,861–12,879.

Sibson, R.H., 1992. Implications for fault-valve behaviour for rupture nucleation and recurrence. Tectonophysics 211, 283–293.

Sibson, R.H., 1998. Brittle failure mode plots for compressional and extensional tectonic regimes. Journal of Structural Geology 20, 655–660.

Sibson, R.H., 2001. Seismogenic framework for hydrothermal transport and ore deposition. Society of Economic Geologists Reviews 14, 25–50.

Sillitoe, R.H., Thompson, J.H.F., 1998. Intrusion-related vein gold deposits: types, tectono-magmatic settings and difficulties of distinction from orogenic gold deposits. Resource Geology 48 (4), 237–250.

Smit, H., Sieb, M., Swanson, C., 1996. The Dublin Gulch project, Yukon Territory. In: Editor, X., (Ed.), Yukon Exploration and Geology 1995, Exploration and Geological Services Division, Yukon, Indian and Northern Affairs, Canada, pp. 33–36.

Smith, M., Thompson, J.F.H., Moore, K.H., Bressler, J.R., Layer, P., Mortensen, J.K., Abe, I., Takaoka, H., 2000. The Leise Zone, Pogo property: a new high-grade gold deposit in Alaska. In: The Tintina Gold Belt: Concepts, Exploration and Discoveries. British Columbia and Yukon Chamber of Mines, Special Volume 2, pp. 131–144.

Stephens, J.R., Weekes, S., 2001. Intrusive breccia-hosted gold mineralization associated with ca. 92 Ma Tombstone Plutonic Suite magmatism: an example from the Bear Paw breccia zone, Clear Creek, Tintina Gold Belt, Yukon. In: Emond, D.S., Weston, L. (Eds.), Yukon Exploration and Geology 2000, Exploration and Geological Services Division, Yukon, Indian and Northern Affairs, Canada, pp. 347–353.

Stephens, J.R., Oliver, N.H.S., Baker, T., Hart, C.J.R., 2000. Structural evolution and controls on gold mineralisation at Clear Creek, Yukon Territory, Canada. In: Emond, D.S., Weston, L. (Eds.), Yukon Exploration and Geology 1999, Exploration and Geological Services Division, Yukon, Indian and Northern Affairs, Canada, pp. 151–163.

Templeman-Kluit, D.J., 1964. Geology of the Haggart Creek–Dublin Gulch area, Mayo district, Yukon Territory. Unpublished Masters Thesis, University of British Columbia, Canada.

Thompson, J.F.H., Newberry, R.J., 2000. Gold deposits related to reduced granitic intrusions. Reviews in Economic Geology 13, 377–400.

Thompson, J.F.H., Sillitoe, R.H., Baker, T., Lang, J.R., Mortenson, J.K., 1999. Intrusion-related gold deposits associated with tungsten–tin provinces. Mineralium Deposita 34, 323–334.

Tosdal, R.M., Richards, J.P., 2001. Magmatic and structural controls on the development of porphyry Cu ± Mo ± Au deposits. Reviews in Economic Geology 14, 157–181.